

# Research on Counting Algorithm of Residual Feeds in Aquaculture Based on Machine Vision

Jiaheng Cao

Department of Control Science and Engineering  
Tongji University  
Shanghai, China  
e-mail: cjhtongji@163.com

Lihong Xu

Department of Control Science and Engineering  
Tongji University  
Shanghai, China  
e-mail: xulhk@163.com

**Abstract**—The waste of feed has always restricted the development of aquaculture. This paper presents an algorithm that can accurately obtain the residual information of feeds after a feeding event. With the purpose of applying the residual feed counting algorithm to the actual production, we focused on solving problems of counting feed pellets, such as turbid pond water, feed adhesion etc. We carry our experiments with different water turbidity levels and with feed adhesion, and some experiments have over 100 pellets. Experiments show that relative error can still be maintained at about 10% under the condition of turbid water and feed adhesion, which is much better than 20% obtained by other counting algorithm.

**Keywords**—feed counting; feed identification; turbid water; dark channel prior; non-uniform illumination

## I. INTRODUCTION

The waste of feed<sup>1</sup> has always been a serious problem in aquaculture. On one hand, the residual feed spawns a big economic loss in the industry because feed accounts for a large proportion of the investment. On the other hand, the residual feed may pollute the water and worsen the living environment of aquatic organisms. The key to solving feed waste problem is to accurately obtain the residual information of the feed and send it to an automatic feeding system. It is applying computer vision to count fish pellet feeds that has become a research focus in recent years, aiming to develop an accurate and reliable detection algorithm for automatic feeding.

Application of computer vision technology in detecting residual feed involves many underwater image processing methods, such as image restoration, image enhancement, image segmentation, and counting. Many scholars have conducted research on underwater image processing. The work by Schechner and Karpel [1] captured two color images of the undersea scene through a polarizing filter to enhance visibility. Although the enhancement is significant, the method is best compatible with horizontal photography rather than acquisitions in the downwards direction. Singh et al. [2] used CLAHE to enhance subsea images, and then

applied the Fuzzy C-Means clustering for segmentation. Schoening et al. Chen et al. [3] proposed an underwater image processing method based on machine learning and achieved better segmentation results for underwater images. Wu [4] proposed an identification method to identify freshwater fish species automatically and accurately, which is based on a multi-kernel least squares support vector machine and artificial bee colony optimization.

Pellet feed detection has drawn attentions from both computer vision and aquaculture engineering communities for quite a time. During a feeding event in a sea cage, Foster et al. [5] observed and counted the falling feed pellets with an underwater camera facing the cage. Ang and Petrell [6] presented some experiments based on indices such as Feed Conversion Ratio (FCR), dispensation rate and so on. Skøien et al. [7] proposed a design based on an integration of Kalman filter and the cost minimization for quantifying feed density in sea cages. Parsonage [8] designed an image processing framework to detect and recognize fish feed pellets with a camera viewing upward for Atlantic salmon cage farming.

## II. PLATFORM AND PROBLEM STATEMENT

### A. Platform

The underwater imaging platform was set up at a fresh water aquaculture site located at Qingpu District of Shanghai, China. The structure of the underwater system is shown in Fig. 1(a) and 1(b). A customized underwater camera (640×480 resolution) with integrated LED lights is fixed to a rod that attached to a thin holder with a height of 1.9 meter. Right below the camera there sits a round plate (effective diameter of 35 cm) which is fixed to the holder. The distance from the camera to the plate is adjustable by changing the connection point of the rod and the top beam of the holder. And it can vary from 20 cm to 50 cm with a step of 3 cm. The underwater system was placed near the daily feeding spot of the pool as the way in Fig. 1(c). Fig. 1(d) shows a little boat that can distribute fish feed pellets, and a worker can use this boat to relocate the underwater imaging system. A video surveillance server was connected to the camera, and underwater videos were stored on the server. The interface of the server is given by Fig. 1(e). After a feeding event, uneaten fish food pellets will remain on the plate.

<sup>1</sup> Feed, diet, feedstuff and forage all indicate food which is used to rear animals in different fields. In this paper, we use *feed* or *feeds* to represent pellet fish food for simplicity.



Figure 1. The underwater imaging platform and the aquaculture site

### B. Feed Counting Problem Statement

During farming, the workers will distribute feed at a fixed time and fixed position [9], and the pellets will remain still in field of view for quite a long time before dissolution. So, we can set fixed-point monitoring in the pond and capture images of the feeds after fish eating. However, there are many difficulties in residual feed counting process, which affect the accuracy of counting.

(1) There are much impurities in ponds due to low frequency of water exchange, excessive delivery of feed, etc. Turbid water will further aggravate the absorption and scattering effects of the water, degrading image contrast and losing details. (2) Due to low illumination, it's necessary to supplement light when acquiring underwater images. And this will cause uneven illumination of captured feed images. (3) During the detection of residual feeds, there may be fish, aquatic grass in captured images. (4) Considering different size of pellets in different breeding stages, use of lifting camera, it's difficult to determine the area of a single pellet feed.

## III. AN IMAGE CLARITY ALGORITHM

### A. Image Dehazing Using Dark Channel Prior

Dark Channel Prior is a statistical rule based on the observation of outdoor haze-free images proposed by Dr. He [10]. In most of the non-sky patches, at least one color channel has some pixels whose intensity are very low and close to zero. The dark channel  $J^{dark}$  of an arbitrary image  $J$  is given by  $J^{dark} = \min_{y \in \Omega(x)} (\min_{c \in \{r,g,b\}} J^c(y))$ , where  $J^c$  is a color channel of  $J$  and  $\Omega(x)$  is a local patch centered at  $x$ . If  $J$  is an outdoor haze-free image, except for the sky region, the intensity of  $J$ 's dark channel is low and tends to be zero:  $J^{dark} \rightarrow 0$ .

A widely used hazy image model can be described as [11], [12]:

$$\mathbf{I}(x) = \mathbf{J}(x)t(x) + \mathbf{A}(1-t(x)) \quad (1)$$

where  $\mathbf{I}$  stands for the observed image,  $\mathbf{J}$  represents the haze-free image,  $\mathbf{A}$  represents the global atmospheric light, and  $t(x)$  is the medium transmission describing the portion of the light that is not scattered and reaches the camera.

Based on dark channel prior and hazy image model, we can roughly estimate  $\tilde{t}(x)$  by

$$\tilde{t}(x) = 1 - \min_{y \in \Omega(x)} \left( \min_{c \in \{r,g,b\}} \frac{I^c(y)}{A^c} \right) \quad (2)$$

But some halos and block artifacts may appear in the recovered image, and we need to refine the rough estimation  $\tilde{t}(x)$ . Considering the efficiency in the refine process, we adopt the guided filter [13] to refine the rough transmission map. And the filtering input image is the rough transmittance map, the guidance image is the grayscale map of the original image.

### B. Underwater Image Restoration

Underwater scene have similar factors in the formation of dark channels in the air [14]. Fig. 2 shows the dark channel maps and histograms of common underwater scenes. It can be found that dark channel maps are black and their histograms concentrated in the bin with very small pixel values. It indicates that dark channel prior is applicable for underwater scenes.

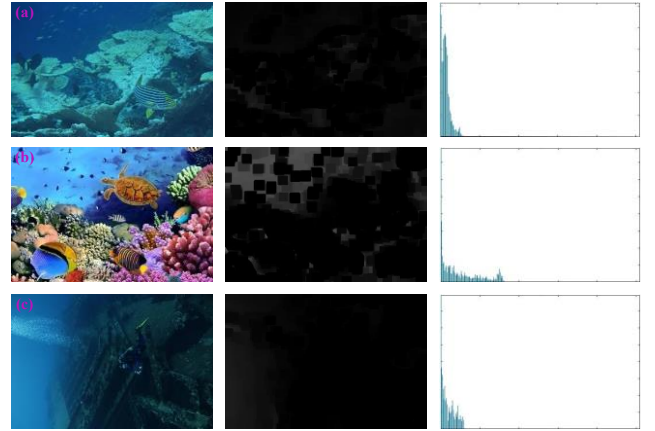


Figure 2. Common underwater images and their dark channel maps and histograms. (a) dark object, (b) colorful marine life, (c) shadow images.

The simplified underwater imaging model can be described as:

$$I_\lambda(x) = J_\lambda(x)t_\lambda(x) + B_{\lambda,\infty}(1-t_\lambda(x)) \quad (3)$$

where  $B_{\lambda,\infty}$  is the global backlight. It can be seen from Eq. (3) and Eq. (1) that underwater imaging model is very similar to the hazy image formation model. Combining that dark channel prior is applicable for underwater scene, we can draw the conclusion that dark channel prior can be used to solve the problem of underwater image blurring and low contrast.

Considering that artificial light resources are applied to the capture of residual feed images, we uses an adaptive method to estimate the background light. We uses a  $(2 * r + 1) \times (2 * r + 1)$  patch in the input image, which centered on the pixel  $(x, y)$  to be restored. And  $r$  is the patch radius. During the restoring process, the patch moves pixel by pixel. First, we select the point with the largest pixel

value of the patch in the dark channel map. Then we select the value corresponding to the selected point in the input image as the background light. Finally, we compare it with the set upper limit ( $A_{up}$ ) and lower limit ( $A_{down}$ ) to determine the background light of  $(x, y)$ . Here we use  $A_{up}$  to limit the background light, thus reduce the brightness caused by artificial light sources, and avoid overcompensation for subsequent steps.

### C. Overview of Image Clarity Algorithm

When the captured feed image does not satisfy the application condition of dark channel prior, we use Contrast Limited Adaptive histogram equalization (CLAHE) [15] to enhance feed images. CLAHE is an variant of the Adaptive Histogram equalization (AHE) [16], which limits the contrast amplification.

Fig. 3 shows the flow of the proposed image clarity algorithm. First of all, we calculate dark channels of the captured images and obtain the median of the dark channels. If the median is lower than the setting threshold, then we obtain the transmission map of the captured image and refine it with guided filter. Next, we choose adaptive background light to restore the image. However, if the median is higher than the threshold, we use CLAHE to enhance the images. During the process, we first enhance R, G and B channel of captured image separately. Then we obtain the average value of each enhanced channel and add modification program to make the enhanced image more normal.

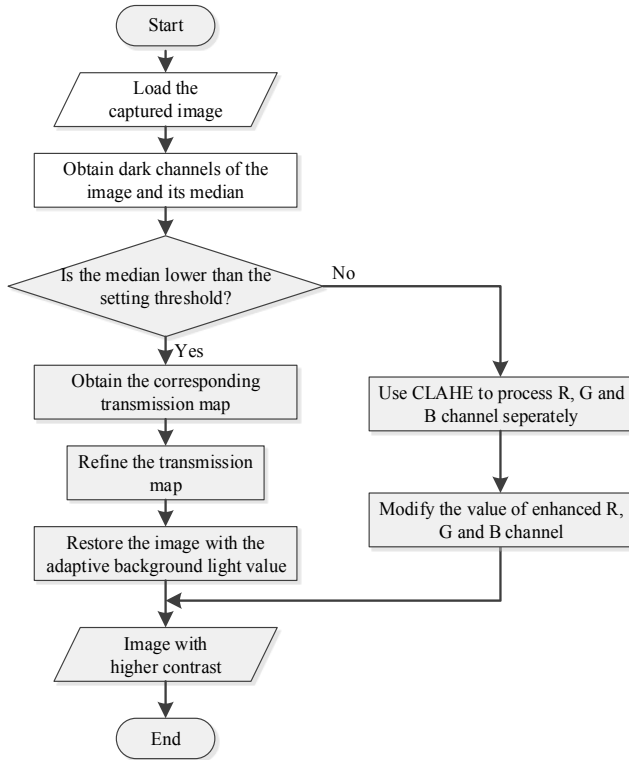


Figure 3. Image clarity algorithm flow chart.

### D. Experiments and Analysis

To show the performance of the proposed method, we choose four common underwater images (see Fig. 4) and two feed images (see Fig. 5). Fig. 4 indicates that our method can make images clearer and avoid being overexposure or dimmer. We further evaluate the restoration result objectively and quantitatively in terms of contrast ratio, information entropy, mean gradient. Table I shows the specific data of the results in Fig. 4 and Fig. 5, from which we can see our method can restore the underwater images to a higher level.

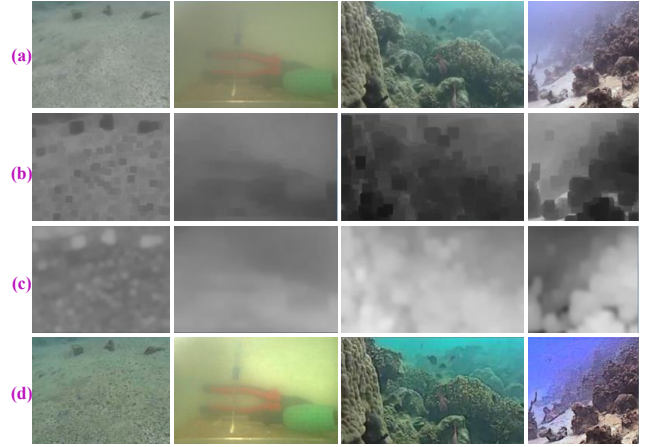


Figure 4. Underwater image restoration. (a) Original underwater image, (b) The corresponding dark channels, (c) The refined transmission maps, (d) Improved images.

TABLE I. QUANTITATIVE EVALUATION OF UNDERWATER SCENE

Scene		scabed	tools	canyon	coral	feed 1	feed 2
Contrast ratio	Original	48.602	4.186	102.341	156.722	2.522	1.437
	Processed	249.727	12.578	206.483	329.397	19.107	12.438
Information entropy	Original	5.613	6.262	7.085	7.393	6.540	6.269
	Processed	6.266	7.322	7.206	7.502	6.644	6.505
Mean gradient	Original	0.022	0.006	0.036	0.047	0.993	0.737
	Processed	0.049	0.010	0.050	0.072	3.037	2.404

Feed images were captured with our experimental platform. We try to simulate the environment of aquaculture ponds as much as possible. During the process, we first crushed the feeds and reconstituted it with water. Then we poured the mixture into the aquarium to simulate the actual fish pond environment.

By comparing the original images and the processed results, it can be seen that the results are brighter. However, it is the details of the image that are of great importance to feed counting. And image (b) shows more and clearer details than the original images in the edge region or other darker regions (see the red region circled in the Fig. 6). These details will benefit binary process and thus bring a more accurate feed counting result. The quantitative evaluation of

the feed images is shown in Table I, which indicates that the proposed method improve the images quality. Image quality improvement contributes to the follow-up residual feed counting algorithm greatly.

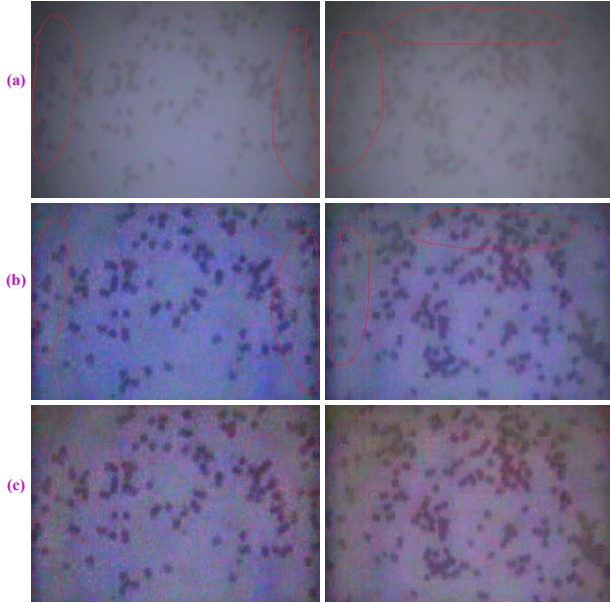


Figure 5. Images of feeds and the processed results. (a) Original feed images, (b) Improved feed images, (c) Images after R, G and B channel modification.

#### IV. COUNTING STRATEGY

We adopt a fast target extraction method to obtain contours of objects. Firstly, we utilize an adaptive thresholding method proposed by Liu et al. [17] to generate the binary feed image, which is based on neighborhood gray value. Secondly, we use Suzuki and Abe's algorithm [18] to find contours of all objects in binary image.

##### A. Finding Area of Single Pellet Feed

To accurately count number of feed heaps, we analyze every contour to judge whether it is a single feed or a feed heap with plenty feed pellets. If it is a feed heap, we use the area-based counting method to further estimate the number of pellets. However, when judging the current contour is a single pellet or a feed heap, estimating the number of pellets of a feed heap, it is an accurate single feed pellet area that are necessary. Because most of the falling feeds are single, we can take the following steps.

Firstly, we set a threshold of contour points to filter out contours with less points in the contour sequence. This aims to remove clastic feeds or floating impurities, which may affect selecting single pellet feed area. Secondly, we calculate each area of the remaining contours and store them in a vector. After sorting the areas according to the order from small to big, we select the median as the area of the single pellet feed. Thirdly, we traverse forward the vector from the middle to 1/4 of the vector in case that there are many feed heaps because of serious feed adhesion. During the traversal, if the area is more than 1.5 times of its previous

one, then take the previous value as area of single pellet feed. Here is the pseudocode of the algorithm.

---

```

1 Determining area of single pellet;
2 int cmin = 20, cmax = 2000;
3 vector<vector<Point>>::const_iterator itc =
  contours.begin();
4 while (itc != contours.end()) do
5   if (itc->size() < cmin or itc->size() > cmax) then
6     erase contour pointed by itc;
7   else
8     itc=itc+1;
9   end if
10 end while
11 vector<double> allArea;
12 for i = 0 to contours.size() do
13   calculate area of current contour, singleArea;
14   allArea.push_back(singleArea);
15 end for
16 sort(allArea.begin(), allArea.end());
17 double median = allArea[allArea.size()/2];
18 for j = allArea.size()/2-1 to allArea.size()/4 do
19   double tmp = allArea[j + 1] / allArea[j];
20   if (tmp > 1.5)
21     median = allArea[j];
22   break;
23 end if
24 end for

```

---

##### B. Estimating Number of Feed Heaps

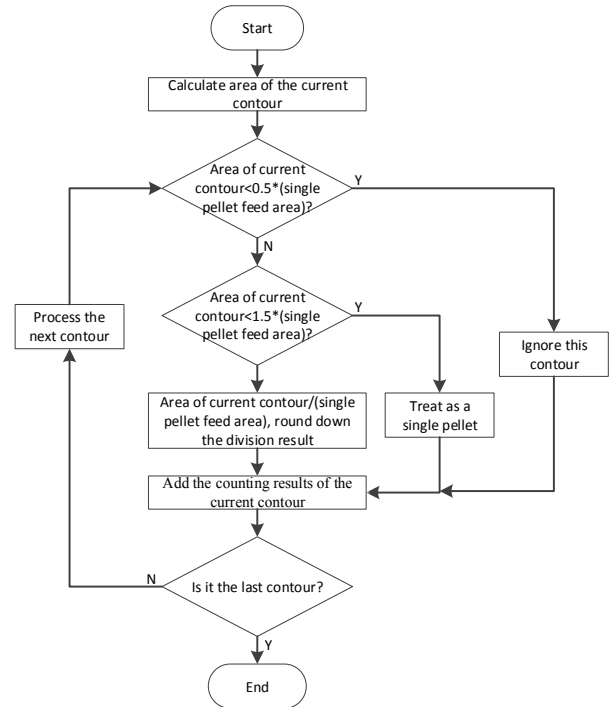


Figure 6. Flow chart of counting strategy



With the area of single pellet feed, we can accurately estimate the number of pellets in feed heaps. When judging whether the current contour is a feed heap or a single pellet feed, we first calculate the area of the current contour and then compare it with the area of a single pellet feed. If the area of the current contour is less than 1.5 times the single pellet area, we treat the current contour as a single pellet. This ratio is mainly to adapt to a slightly bigger pellet feed than the selected median, but small enough to make it less likely that it contains feed adhesion. If the area of the current contour is less than 0.5 times the single pellet area, we treat the current contour as clastic feeds. The remaining contours are treated as feed heaps. For these contours, we divide their areas by the single pellet area and take the approximation as numbers of feed pellets. (The approximation indicates rounding down the division result.) Finally, we can obtain the number of pellet feeds in captured image by summarizing the counting results of all the contours. Fig. 6 shows the flow chart of the counting strategy.

### C. Experiments and Analysis

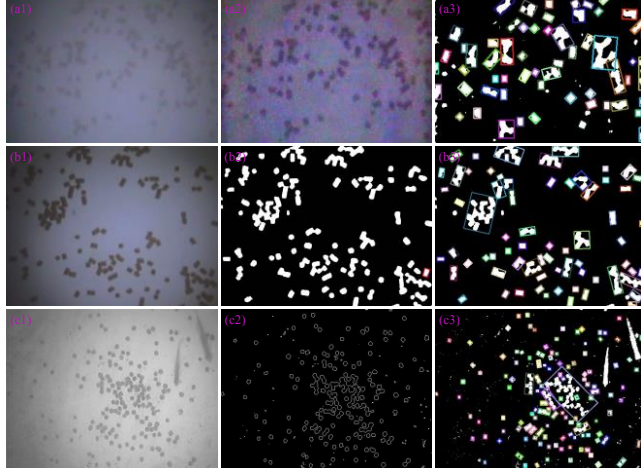


Figure 7. Counting results. (a1) Image captured in turbid water, (a2) Improved image, (b1) Image of feed piles, (b2) Selected single pellet (bounded by red rectangle), (c1) Image containing non-bait object, (c2) Image of contours after removing fishes, (a3) (b3) (c3) Labeled images corresponding to first column.

Considering various feed images captured in practical production, we chose three groups of typical feed images, which correspond to capture conditions like turbid water, feed adhesion, and non-feed object interference. Each group includes three different images so as to prove the accuracy of the proposed algorithm. Fig. 7 shows the intermediate images and labeled images of three typical feed images. And we use random color to mark the feed contours in counting process, which are shown in the labeled images in 3<sup>rd</sup> column. Comparing Fig. 7(a1) captured in turbid water with Fig. 7(a2) improved by the method in section 3, it can be found that (a2) is the brighter than (a1) and (a2) shows more details than (a1). The blur edges of (a1) are still difficult to count manually. However, the labeled image (a3) indicates that our algorithm accurately labelled and counted the pellet feeds except those from the edges, whose area are less than half of

the single pellet. Although there are more feed piles in Fig. 7(b1). The single pellet feed is marked with a red rectangle in the lower right corner of (b2). And the feed piles are accurately marked and counted (see Fig. 7(b3)). Foraging fishes in Fig. 7(c1) are accurately eliminated (see Fig. 7(b2)). Thus are not taken as feeds in Fig. 7(b3).

Table II shows the statistical result of the counting algorithm [19] without considering the actual situations like turbid pond water and feed adhesion. Image 1, 2, and 6 are ideal images captured in clear water, and there is almost no feed adhesion. However, when the water gets turbid and feed adhesion appears, the relative error also increases.

TABLE II. RESULT OF ALGORITHM WITHOUT CONSIDERING TURBIDITY AND ADHESION

Image Description	Ideal	Ideal	Turbid and Adhesion	Adhesion	Turbid	Ideal
Image ID	1	2	3	4	5	6
Statistical quantity	42	23	34	96	78	51
Actual quantity	44	25	43	118	92	55
Relative error	4.76%	8%	20.93%	18.64%	15.22%	7.27%

Table III shows the results of our algorithm with nine different feed images, including the statistical quantity, actual quantity, and relative error of each one. The actual quantity of chosen images range from 41 to 178, and five images include more than 100 pellets. It's more fit the reality in the actual production. In the experiments, statistical quantities of figure (d), (e) and (g) are larger than their actual quantities. Because there are too many feeds in these image more large feed piles.

In short, relative error can be controlled around 10% when counting most of the feed images by our algorithm. And only a small portion of feed images has higher relative error, which may be captured in very turbid water. It indicates that the proposed feed counting algorithm can meet the accuracy requirements of the automatic feeding control system and can be applied to practical production. By comparison, we can find that our counting algorithm can effectively reduce the relative error under various conditions.

TABLE III. COUNTING RESULTS OF OUR ALGORITHM

Image description	Ideal	Turbidity		Non-feed interference			Adhesion		
Image ID	a	b	c	d	e	f	g	h	i
Statistical quantity	39	124	90	184	125	94	119	36	66
Actual quantity	41	140	95	178	116	104	113	40	73
Relative error	4.88%	11.43%	5.26%	3.37%	7.76%	9.62%	7.96%	10%	9.59%

## V. DISCUSSION

In this paper, we have proposed an residual feed counting algorithm, which is proved both accurate and reliable by

various experiments. The algorithm solves problems commonly encountered in feed counting from actual production, and can be applied to turbid underwater environments. It can meet the precision requirements of the automatic feeding control system and can be applied to practical production.

However, due to time constraints and the complexity of feed counting, residual feed counting algorithm still have some problems and deficiencies, which are as follows. (1)When segmenting the non-feed object, the feeds connected to the non-feed object contours are also removed. And we haven't got a valid strategy to estimate quantity of feeds sheltered by non-feed object. (2)We haven't consider whether small feed scraps need to be counted, or how to be counted. (3)When using area-based method to estimate the number of feed piles, gaps between the feeds are taken as feeds, resulting in a larger statistical quantity than the actual quantity.

#### ACKNOWLEDGEMENT

This work was supported in part by National Key R&D Plan under Grant 2017YFD0701700, the National Natural Science Foundation of China under Grant 61573258 and in part by the U.S. National Science Foundation's BEACON Center for the Study of Evolution in Action, funded under Cooperative Agreement DBI-0939454.

#### REFERENCES

- [1] Y. Y. Schechner and N. Karpel, "Recovery of underwater visibility and structure by polarization analysis," *IEEE J. Ocean. Eng.*, vol. 30, no. 3, pp. 570–587, 2006.
- [2] S. Singh, M. Soni, and R. S. Mishra, "Segmentation of Underwater Objects using CLAHE Enhancement and Thresholding with 3-class Fuzzy C-Means Clustering."
- [3] Z. Chen, H. Wang, L. Xu, and J. Shen, "Visual-adaptation-mechanism based underwater object extraction," *Opt. Laser Technol.*, vol. 56, no. 1, pp. 119–130, 2014.
- [4] Y. Wu, J. Yin, Y. Dai, and M. Yuan, "Identification method of freshwater fish species using multi-kernel support vector machine with bee colony optimization," *Transactions of the Chinese Society of Agricultural Engineering*, vol. 30, no. 16, pp. 312–319, 2014.
- [5] M. Foster, R. Petrell, M. R. Ito, and R. Ward, "Detection and counting of uneaten food pellets in a sea cage using image analysis," *Aquac. Eng.*, vol. 14, no. 3, pp. 251–269, 1995.
- [6] K. P. Ang and R. J. Petrell, "Control of feed dispensation in seacages using underwater video monitoring: Effects on growth and food conversion," *Aquac. Eng.*, vol. 16, no. 1, pp. 45–62, 1997.
- [7] K. R. Skøien, M. O. Alver, and J. A. Alfredsén, "A computer vision approach for detection and quantification of feed particles in marine fish farms," in *IEEE International Conference on Image Processing*, 2015, pp. 1648–1652.
- [8] K. D. Parsonage, "Detection of fish-food pellets in highly-cluttered underwater images with variable illumination," 2001.
- [9] H. Wang, "How to do well in the middle and later periods of rearing fish," *Heilongjiang Fisheries*, no. 4, pp. 25–27, 2013.
- [10] K. He, J. Sun, and X. Tang, "Single Image Haze Removal Using Dark Channel Prior," *IEEE Trans. Pattern Anal. Mach. Intell.*, vol. 33, no. 12, pp. 2341–2353, 2011.
- [11] S. G. Narasimhan and S. K. Nayar, "Vision and the Atmosphere," *Int. J. Comput. Vis.*, vol. 48, no. 3, pp. 233–254, 2002.
- [12] R. Fattal, "Single image dehazing," in *Acm Siggraph*, 2008, pp. 1–9.
- [13] K. He, J. Sun, and X. Tang, "Guided image filtering," *IEEE Trans. Pattern Anal. Mach. Intell.*, vol. 35, no. 6, pp. 1397–1409, 2013.
- [14] M. M. Cheng, G. X. Zhang, N. J. Mitra, X. Huang, and S. M. Hu, "Global contrast based salient region detection," in *Computer Vision and Pattern Recognition*, 2011, pp. 409–416.
- [15] K. Zuiderveld, Contrast limited adaptive histogram equalization. Academic Press Professional, Inc., 1994.
- [16] A. M. Reza, "Realization of the Contrast Limited Adaptive Histogram Equalization (CLAHE) for Real-Time Image Enhancement," *J. Vlsi Signal Process. Syst. Signal Image Video Technol.*, vol. 38, no. 1, pp. 35–44, 2004.
- [17] H. Liu and L. Xu, "Detection and recognition of uneaten fish food pellets in aquaculture using image processing," in *International Conference on Graphic and Image Processing*, 2015, p. 94430G–94430G–7.
- [18] S. Suzuki and K. Be, "Topological structural analysis of digitized binary images by border following," *Comput. Vis. Graph. Image Process.*, vol. 30, no. 1, pp. 32–46, 1985.
- [19] H. Liu, "Image-based Underwater Fish Food Detection for Automatic Feeding in Aquaculture," Tongji University, 2015.